JOC The Journal of Organic Chemistry

Article

pubs.acs.org/joc

Selective Modulation of Internal Charge Transfer and Photoinduced Electron Transfer Processes in *N*-Aryl-1,8-Naphthalimide Derivatives: Applications in Reaction-Based Fluorogenic Sensing of Sulfide

Ranjith K. Meka and Michael D. Heagy*

Department of Chemistry, New Mexico Institute of Mining & Technology, Socorro, New Mexico 87801, United States

Supporting Information

ABSTRACT: Three reaction-based fluorescent probes based on two new naphthalimide platforms were developed for the detection of H_2S. A new approach in detecting H_2S by the reduction of an azide to a triazene intermediate in aqueous media is reported. Given their design features, these chemodosimeters provide useful insights into the relatively unexplored area of C_0 spacers between receptor:reporter components. The *N*-aryl-1,8-naphthalimide platform features straightforward placement of the internal charge transfer and photoinduced electron transfer (PET) modulators on the same molecule. In the three examples presented, the *N*-aryl component proved to be an effective photophysical device as it allows the placement of a PET modulator at the strategically important and less explored imide position of 1,8-naphthalimides. These probes or dosimetric agents demonstrated good selectivity, two-signal response, and the desirable OFF−ON fluorescence response. By implementation of both the azido and nitro group as sulfide-reactive functionalities on the same chemosensory platform in probe SNAN-3, a much broader range of H_2S can be detected. Remarkably, probe SNAN-3 exhibits both a dual-emission and dual-response for the detection of sulfide in aqueous solution.

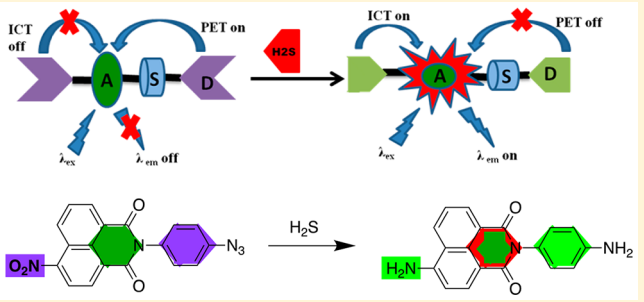

INTRODUCTION

Hydrogen sulfide (H_2S) is the most recently discovered gasotransmitter among the known other endogenous gases nitric oxide (NO) and carbon monoxide (CO).[1−6] Upon endogenous production through various biosynthetic, enzymatic, and nonenzymatic processes, H_2S plays a pivotal role in nervous, immune, endocrine, and cardiovascular systems.[7] In cells, abnormality in the levels of H_2S has been associated with many pathological conditions such as Alzheimer's disease, liver cirrhosis, and arterial/pulmonary hypertension.[8] However, H_2S has a distinct rotten egg smell and is known to be comparably toxic to HCN or CO gases.[9,10] In addition, under anoxic environments, H_2S controls the bioavailability of several heavy metals.[11] Therefore, measuring accurate concentrations of H_2S is critical in understanding its physiological, pathological, and environmental importance. Several analytical techniques such as colorimetric[12,13] and electrochemical assays,[14,15] gas chromatography,[16,17] and metal-induced sulfide precipitation[18] were reported for the measurement of endogenous H_2S concentrations. However, most of these techniques require various pretreatment procedures, and thus, variable H_2S concentrations were reported ranging from nano- to milli-molar levels.[19−21] The design of chemodosimeters for H_2S based on fluorescence modulation has emerged as a major analytical technique in cell biology, medicine, environmental chemistry, and material science. Due to the high reactivity of the endogenously produced sulfide, several reaction-based fluorescent probes (chemodosimeters) have emerged for its detection.[22,23] Among these chemosensory systems, the reduction of an aromatic azide group to an amine by H_2S has been utilized extensively because of the bio-orthogonality of the reaction and associated electronic changes in the probe.[24−28] Because of their modular synthesis, the 1,8-naphthalimide-based fluorescent probes have prompted considerable research in optical imaging and detection.[29−33] By the innovative use of the sulfide's nucleophilic and consequential reducing properties, several of these probes were employed in detecting environmental,[34] cellular,[35−39] and intracellular sulfide.[40]

The naphthalimide platform offers sensitive modulation of fluorescence properties (based on changes in position 4), and good quantum yields. Naphthalimide dyes can be synthetically manipulated into a reporter that exhibits either photoinduced electron transfer (PET) or internal charge transfer (ICT).[41] As a PET-based chemodosimeter, the naphthalimide can be designed as a fluorophore-spacer-modulator.[42−45] In such systems, the C_n spacer can be a short aliphatic chain; alternatively, in an *N*-aryl-1,8-naphthalimides, virtual C_0 spacer systems occur with a phenyl ring at the *N*-imide position platform. In either case, the spacer separates electronic interactions and impedes charge recombination between the fluorophore/transducer and the receptor/modulator to the ground state. In contrast to these architectures, the dipolar nature of an electron-rich aromatic fused to an imide functionality can be augmented by conjugation with polar groups at the 4-position to generate a

Received: August 3, 2017
Published: November 1, 2017

DOI: 10.1021/acs.joc.7b01952
J. Org. Chem. 2017, 82, 12153−12161

chemodosimeter capable of exhibiting a photoinduced internal charge transfer (ICT) state. The most prominent difference between PET and ICT-based chemodosimeters lies in the different fluorescence responses upon analyte reaction. PET chemodosimeters display enhancement or quenching of fluorescence without pronounced spectral shifts, so the intensiometric terms OFF−ON or ON−OFF fluorescent sensors apply. Such designs are ruled out for potential ratiometric detection at two different wavelengths. On the other hand, chemodosimeters based on ICT pathways show clear fluorescence maximal shifts upon sulfide detection, making ratiometric measurements possible. Because the naphthalimide framework allows for both designs, a more sophisticated and thorough approach would involve the combination of both the PET and ICT processes into a single molecule.

On the basis of modulated 1,8-naphthalimide scaffolds, Figure 1 illustrates three different chemodosimetric approaches

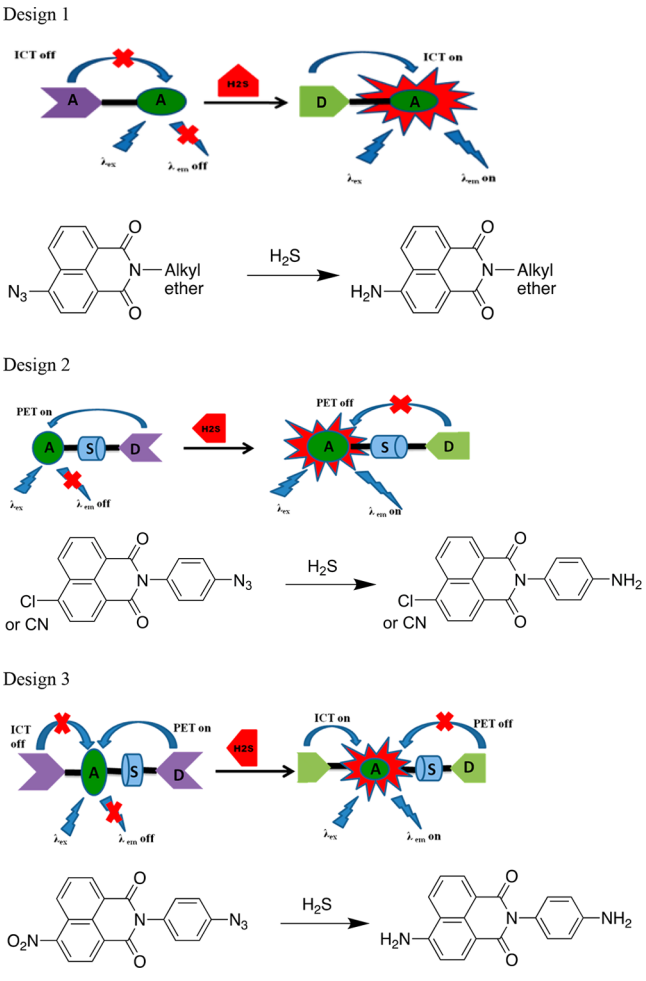

Figure 1. Three different reaction-based design strategies for the sensing of sulfide. Examples of design 1 have been previously reported.[35,41−44] This work investigates designs 2 and 3 and their reaction-based emission behavior (A = acceptor, S = spacer, and D = donor).

to generate either ICT or PET processes for sensing sulfide. As shown in design 1 (Figure 1), most of these probes take advantage of the ICT process resulting from the conversion of an electron-withdrawing group (−NO_2, −N_3, and −NHOH), located at position 4, to an electron-releasing group (−NH_2).[46] However, no studies have ventured to compare both a nitro group and azido group and their corresponding sulfide reactivities on the same fluorescent molecule. In this work, we explored the consequences of modulating either the PET process (design 2, Figure 1) or in an unprecedented example, both the PET and ICT processes (design 3, Figure 1) in 1,8-naphthalimide-based chemodosimeters for sensing sulfide. Here, we report a group of fluorogenic reaction-based 1,8-naphthalimide probes for the detection of sulfide that modulate the fluorescence response caused by *N*-aryl contributions.

RESULTS AND DISCUSSION

Established by our group and others, the electronic contributions from the *N*-aryl substituents play an important role in governing the fluorescent properties of *N*-aryl-1,8-naphthalimides.[47−50] Due to their near orthogonality in solution,[51] there is a negligible interaction between the *N*-aryl ring and the naphthalimide fluorophore in the ground state. This creates a unique orthogonal orbital system that allows the connection of donors to the imide nitrogen without a bridge (i.e., a virtual C_0 spacer) and modulation of the fluorescent properties via the PET process. According to our seesaw model, if an electron-withdrawing group is present on the naphthalimide ring (position 4), depending on the nature of the group present on the *N*-aryl ring, i.e. either electron-withdrawing group (EWG) or donating group (EDG), a unique fluorescence response is predicted.[52,53] If an EWG is appended, only a single fluorescence maxima at shorter wavelength results, whereas if an EDG is appended, a dual fluorescence response at short and long wavelengths is observed. Therefore, we reasoned that a system with synthetic placement of the azido group as the EDG on the *N*-aryl ring with an electron-withdrawing group on the naphthalimide should also serve as a tool in understanding the mechanism of azide reduction by sulfide.

The synthesis of the designed probes is illustrated in Scheme 1. 4-Chloro and 4-cyano-1,8-naphthalic anhydrides were chosen as they exhibited dual fluorescence upon substitution of the *N*-aryl component with a *para*-amino group. Both the 4-chloro-1,8-naphthalimide and 4-nitro-1,8-naphthalimide were commercially available, whereas the 4-cyano-1,8-naphthalimde was prepared via treatment of 4-bromo-1,8-naphthalimide with CuCN in DMF. As shown in Scheme 1, different 4-substituted 1,8-naphthalic anhydrides were treated with *p*-phenylenediamine in ethanol under reflux to obtain *N*-aryl-1,8-naphthalimides.[54,55] The *para*-amino group was then diazotized and treated with sodium azide to obtain *N*-aryl azido-1,8-naphthalimide probes via nucleophilic aromatic substitution.[56,57] Percent yields are reported in overall amounts for each SNAN derivative.

Among the reaction-based probes that utilized the azide group reduction to detect sulfide, as mentioned above, the formation of an amine product was reported. This functional group transformation proved to be advantageous for modulation of the fluorescent signal. In light of these findings and our earlier observations, we anticipated that these probes would exhibit dual fluorescence upon the reduction of the azide group on the *N*-aryl ring.[58,59] Yet, compared to other azide probes, the amines of **4**, **5**, and **6** (Scheme 1) exhibited weak fluorescence in 5% DMSO in PBS (pH 7.4) solution (Supporting Information). Furthermore, to our surprise, upon the treatment of either 30 μM SNAN-1 or SNAN-2 with 30 μM NaSH (used as H_2S equivalent in solution), in 2 h, a 6- and 7-fold OFF−ON response at 408 and 410 nm was observed, respectively (Figure 2).

The detection limit of SNAN-1,2 for H_2S after 120 min incubation was found to be between 0.1 and 0.5 μM (Supporting Information). This change in fluorescence intensity with minimal

DOI: 10.1021/acs.joc.7b01952
J. Org. Chem. 2017, 82, 12153−12161

Scheme 1. General Synthetic Scheme for the Synthesis of Probes SNAN-1, 2, and 3

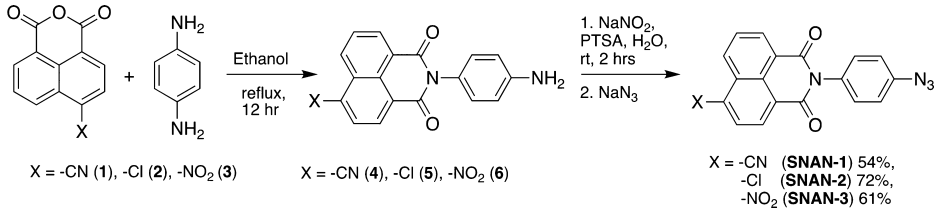

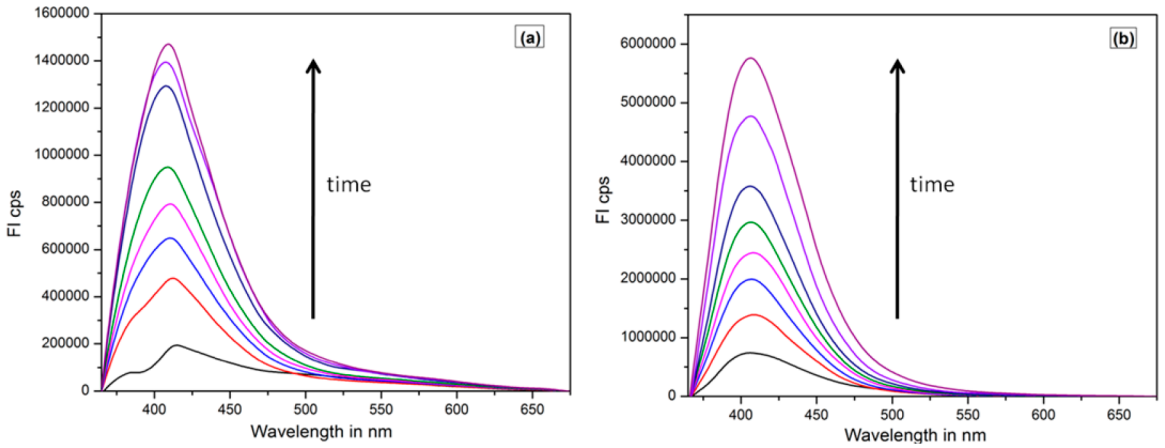

Figure 2. Fluorescence enhancement of SNAN-1 and SNAN-2 upon added sulfide: (a) 30 μM SNAN-1 and (b) 30 μM SNAN-2 after adding 30 μM H_2S. Data were acquired in 95:5 1× PBS (pH 7.4):DMSO with λ_{ex} = 350 nm. Emission intensity was collected between 365 and 675 nm. Time points represent 0, 10, 20, 30, 40, 60, 90, and 120 min after H_2S addition.

Scheme 2. Azide to Amine Transformation Mechanism Invoking Triazene Intermediate Responsible for PET Modulation in SNAN Probes

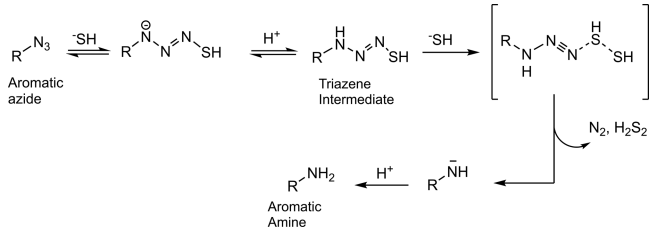

or no change in fluorescent wavelength is the signature optical response of PET-based quenching.[60−63] In 1,8-naphthalimides,[47,51] it was shown that if an electron-donating substituent is connected to the imide nitrogen (in conjugation through an aryl group), they act as PET donors and quench the fluorescence of the naphthalimide acceptor. In addition, it was also established that in many fluorophores, the azide group quenches fluorescence through the PET process.[24] Thus, the differences in the fluorescence intensities of the amines (**4** and **5**) with the azide probes (SNAN-1 and SNAN-2) could be due to the differences in quenching ability of the respective groups. Interestingly, in our case, we were able to confirm experimentally that the amine group is a better quencher of fluorescence than the azide group via the PET process.

Perhaps more significantly, we observed an increase in fluorescence quantum yield while using the probes SNAN-1 and SNAN-2 to detect H_2S. This suggests that during the reduction of the azide group by sulfide, an intermediate group is formed that has lower quenching efficiency compared to either the azide or the amine groups. Therefore, we attribute this long-lived or relatively stable intermediate to the observed increase in fluorescence quantum yield. In the case of SNAN-1, the signal intensity starts decreasing after 5 h, indicating that the intermediate slowly converts to the more thermodynamically stable amine product and results in PET quenching. By comparison, the intermediate for SNAN-2 was found to be more stable as the quenching of fluorescence is observed only after 12 h. To further substantiate the evidence for the occurrence of the PET process, a fluorescence study was conducted by protonating the amines (**4** and **5**) under acidic conditions (Supporting Information). This resulted in a dramatic increase in the fluorescent signal intensity of the amine compounds without a change in their emissive maxima (Supporting Information). Because both of the aforementioned observations led to an increase in the same emissive maxima, it can be reasoned that PET quenching is the operative mechanism.

To identify the reaction intermediate, an NMR study of SNAN-2 with 1.5 equiv of NaSH in DMSO-d_6:CD_3OD (50:50) was conducted (Supporting Information). Upon the addition of NaSH, the *N*-aryl ^1H signals undergo a dramatic shift, indicating the reduction of azide group is fast (<5 min). A new peak at 9.14 ppm was formed which gradually increased with time. In light of the reported[61] mechanistic insights in H_2S mediated reduction aryl azides, we reasoned that the addition of NaSH to

DOI: 10.1021/acs.joc.7b01952
J. Org. Chem. 2017, 82, 12153−12161

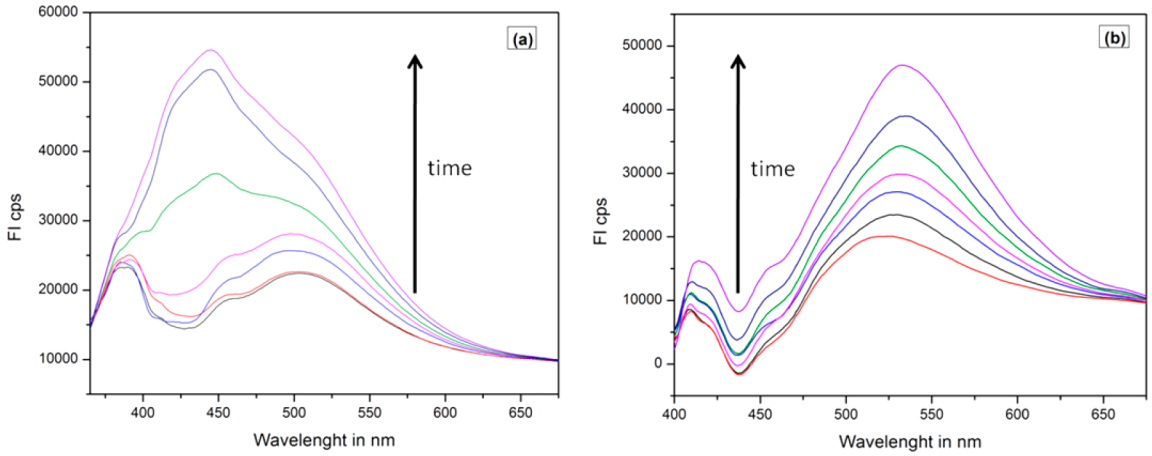

Figure 3. Fluorescence enhancement of SNAN-3 with H_2S: (a) 0.5 μM and (b) 50 μM H_2S with 5 μM SNAN-3. Data were acquired in 90:10 1× PBS (pH 7.4):DMSO with λ_{ex} = 350 nm. Emission intensity was collected between 365 and 675 nm. Time points represent 15, 30, 45, 60, 90, 120, and 180 min after H_2S addition.

SNAN-2 resulted in the formation of a triazene intermediate before converting to a more thermodynamically stable amine product. In addition, according to our photophysical model,[52,53] placing electron withdrawing groups on both *N*-aryl and naphthalimide moieties results in short wavelength emission. This similar observation for SNAN-2 further substantiates the evidence of an observed NMR signal at 9.14 ppm, which can be attributed to the −NH proton from the intermediate triazene.[35] Here, we report for the first time the use of such an intermediate group to detect H_2S.

On the basis of our observations in sensing sulfide with SNAN-1 and SNAN-2 along with comparisons drawn from the comprehensive study by Pluth et al.,[61] a sensing mechanism is shown in Scheme 2 where the R-group represents the 1,8-naphthalic platform. The long-lived intermediate generated by SNAN-2 corroborates their mechanistic evidence whereby a two-step and two-equivalent H_2S pathway favors a fast, first-step conversion to the analogous triazene intermediate derived from 4-methyl-7-azidocoumarin. Here, a higher energy of activation ($\Delta H_2^{\ddagger}$) and consequently rate-determining second-step indicates a local energy minima for this intermediate to reside along the reaction coordinate. Intrigued by our observations involving the PET modulation to detect H_2S and the already established ICT modulation,[35−38] we integrated both of these processes for 1,8-naphthalimides. Moreover, due to orbital orthogonality between the naphthalimide fluorophore and the *N*-aryl group,[51−53] the *N*-aryl substituents modulate only the PET process but not the ICT process.[58−60,62] Because both of these processes exhibit two different emission and excitation wavelengths, it is possible to increase the signal diversity and promote either PET or ICT responses.[63] Such a response can be useful in mitigating the disadvantages associated with a single intensiometric response.[64,65] To the best of our knowledge, no such chemodosimetric probes exists for the detection of H_2S. Consequently, we designed and synthesized probe SNAN-3.

As established above, the azide group on the *N*-aryl ring can be reduced to a triazene intermediate to obtain a fluorogenic response. Also, the nitro group in position 4 of the 1,8-naphthalimide can be reduced to an amino group to obtain a fluorogenic response.[46] However, there are known reactivity and sensitivity differences between the azide and the nitro groups. As reported by Montoya et al.,[35] under the same chemical environment, the azide group reacts at a much faster rate and is more sensitive toward sulfide than the nitro group. On the other hand, in SNAN-3, the two reactive groups, the 4-NO_2 and the *N*-aryl azido, are appended to different aromatic components, i.e. chemical environments. Therefore, it was important to establish the sensitivity and selectivity of both groups to gain a mechanistic understanding of the detection of sulfide by SNAN-3. By considering the detection limits shown by SNAN-1 and SNAN-2, two different assay conditions were designed for SNAN-3. In one assay, the sulfide concentrations were limited by sulfide concentration at 0.1 equiv of H_2S to 1 equiv of SNAN-3, and in the other assay, 1 equiv of H_2S to 0.1 equiv of SNAN-3.

The fluorescence responses obtained are shown in Figure 3. Under the sulfide limiting conditions (Figure 3a), the fluorescence spectra remained broad between 365 to 525 nm and after 120 min showed a maximum at 445 nm with a 4-fold OFF−ON response. In comparison, similar to the probes SNAN-1 and SNAN-2, the intermediate formed in the reaction of SNAN-3 with sulfide showed fluorescence quantum yield higher than that of the corresponding aromatic amine (Scheme 2). Under the aforementioned conditions, the signal intensity is modulated only by the PET process, which demonstrates that the azide group's sensitivity remains higher than that of the nitro group. The PET signal intensity, however, starts decreasing after 3 h, indicating the formation of amine product. Thus, it appears that the observed differences in the fluorescence turn on ratios are due to the differences in the half-life of the SNAN probe's sulfide reaction intermediates. ^{1}H NMR evidence for the long-lived intermediate in the reduction of SNAN-2 is reported in the Supporting Information. Such differences are a consequence of the electron withdrawing nature of the substituents present on the 1,8-naphthalimide. Lastly, in the case of SNAN-3, additional quenching is possible due to the known quenching ability of the nitro group.[65]

Under the probe limiting conditions (10 equiv of H_2S to probe ratio), we see the conversion of both the azido and the nitro groups to the diamine product (compound 7, Scheme 3). Upon excitation at 350 nm, two emission bands centered at 410 and 540 nm are observed with two and 4-fold turn ON response, respectively (Figure 3b). It is apparent under these conditions that the formed ICT donor amine group in position 4 of the 1,8-naphthalimde platform determines the emission spectrum. During the assay, it was observed that a bathochromic shift of

DOI: 10.1021/acs.joc.7b01952
J. Org. Chem. 2017, 82, 12153−12161

Scheme 3. Treatment of SNAN-3 under H_2S-Limiting Conditions (0.1 equiv) and Probe-Limiting Conditions (10 equiv H_2S)

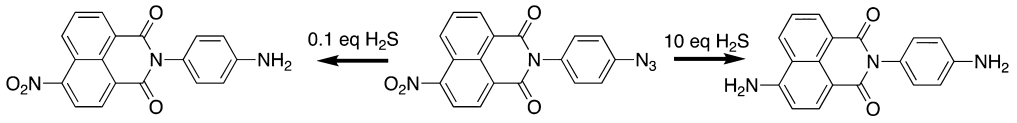

6 SNAN-3 7

Table 1. Spectroscopic Data for SNAN-1, SNAN-2, and SNAN-3 Probes Only with H_2S and Corresponding aAmines 4, 5, 6, and 7

entry	compound	λ_{max} abs (nm)	ε (M^{-1} cm^{-1})	λ_{max} fl. 1 (nm) SW	λ_{max} fl. 2 (nm) LW	Φ^d SW Fl. 1 ($\times 10^{-4}$)	Φ^d LW Fl. 2 ($\times 10^{-4}$)
1	SNAN-1	350	8814	409		2.94	
2	**4**	350	9756	412		0.32	
3	SNAN-1 with H_2S^a	350		408		14.4	
4	SNAN-2	350	7551	408		9.56	
5	**5**	347	6149	397		2.93	
6	SNAN-2 with H_2S^a	350		410		58.8	
7	SNAN-3	350	5256	410		3.98	
8	**6**	352	6000	454		0.981	
9	SNAN-3 with H_2S^b	350		445		5.45	
10	7	436	13372	410[c]	540[c]	15.6[c]	58.6[c]

[a]1 to 1 equiv of probe with H_2S (30 μM). [b]1 to 0.1 equiv of probe with H_2S (0.5 μM). [c]Upon excitation at 350 nm. [d]Quantum yields are in reference to quinine sulfate (Φ = 0.577 in 0.05 N H_2SO_4).

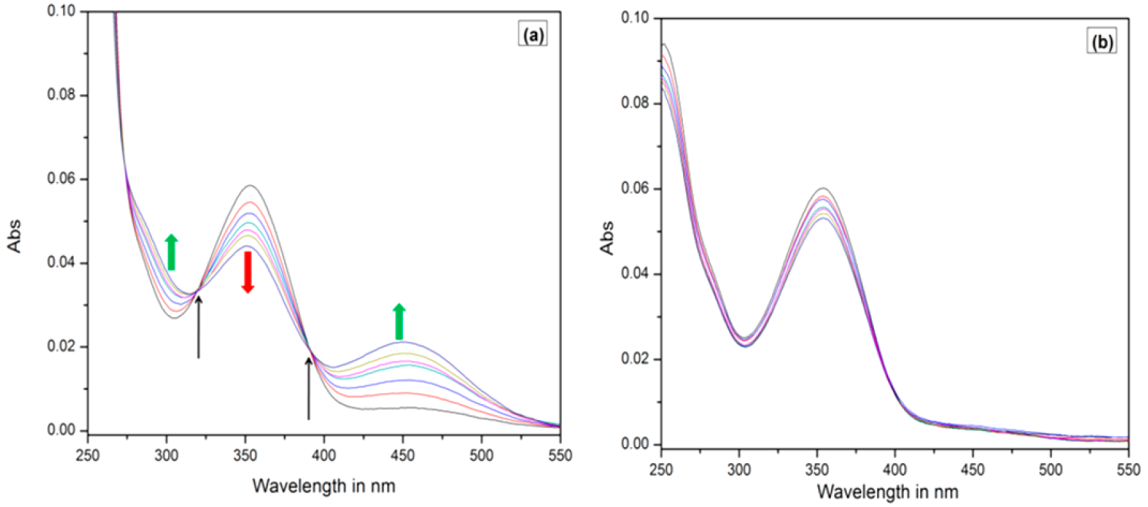

Figure 4. Absorbance spectra of SNAN-3 with H_2S: (a) 500 μM and (b) 0.5 μM H_2S with 5 μM SNAN-3. Data were acquired in 90:10 1× PBS (pH 7.4):DMSO. Time points represent 15, 30, 45, 60, 90, 120, and 180 min after H_2S addition. The arrows (green = increase, red = decrease, and black arrows = isosbestic points) indicate changes in the spectrum at corresponding wavelengths).

10 nm of the spectrum occurs during the first hour which, in the case of other fluorophores, is typically attributed to the concentration effects.[67] However, the differences in the OFF to ON ratios between previously reported HSN1 probe[35] and SNAN-3 can be attributed to the differences in excitation wavelengths, i.e. 350 nm for SNAN-3 as opposed to observed λ_{max} of 436 nm for compound **7**, the final product formed from sulfide reduction of SNAN-3. The possibility of PET quenching the fluorescence due to the formation of *N*-aryl amine product as shown in the cases of compounds **4** and **5** may also contribute to the observed differences. Furthermore, an increase in the rate of internal conversion due to changing the *N*-alkyl group to a *N*-phenyl group[66−68] may cause further decreases in fluorescence turn-on ratios. Table 1 summarizes the optical features of all SNAN-1,2,3 azides and corresponding sulfide reduced species.

At this point, it should also be noted that the sulfide concentrations used to generate the turn-on response also differ considerably. The detection limit of SNAN-3 for H_2S after 120 min incubation was found between 0.1 and 0.5 μM based on azide group reduction, i.e. for the PET-based modulation of fluorescent signal (Supporting Information). The detection limit for the ICT-based modulation of fluorescent signal remains the same as that reported earlier,[35] i.e. between 5 and 10 μM. To the best of our knowledge, SNAN-3 is the first example showing two unique responses at two different concentrations of H_2S. Moreover, compared to the reported nitro, azido reduction probes HSN1, HSN2,[35] and hydroxyl amine reduction probe,[37] SNAN-3 not only improved the detection limit but also increased the signal diversity.

To substantiate the evidence for the aforementioned selective PET and ICT modulations, the absorption spectra of the assay

DOI: 10.1021/acs.joc.7b01952
J. Org. Chem. 2017, 82, 12153−12161

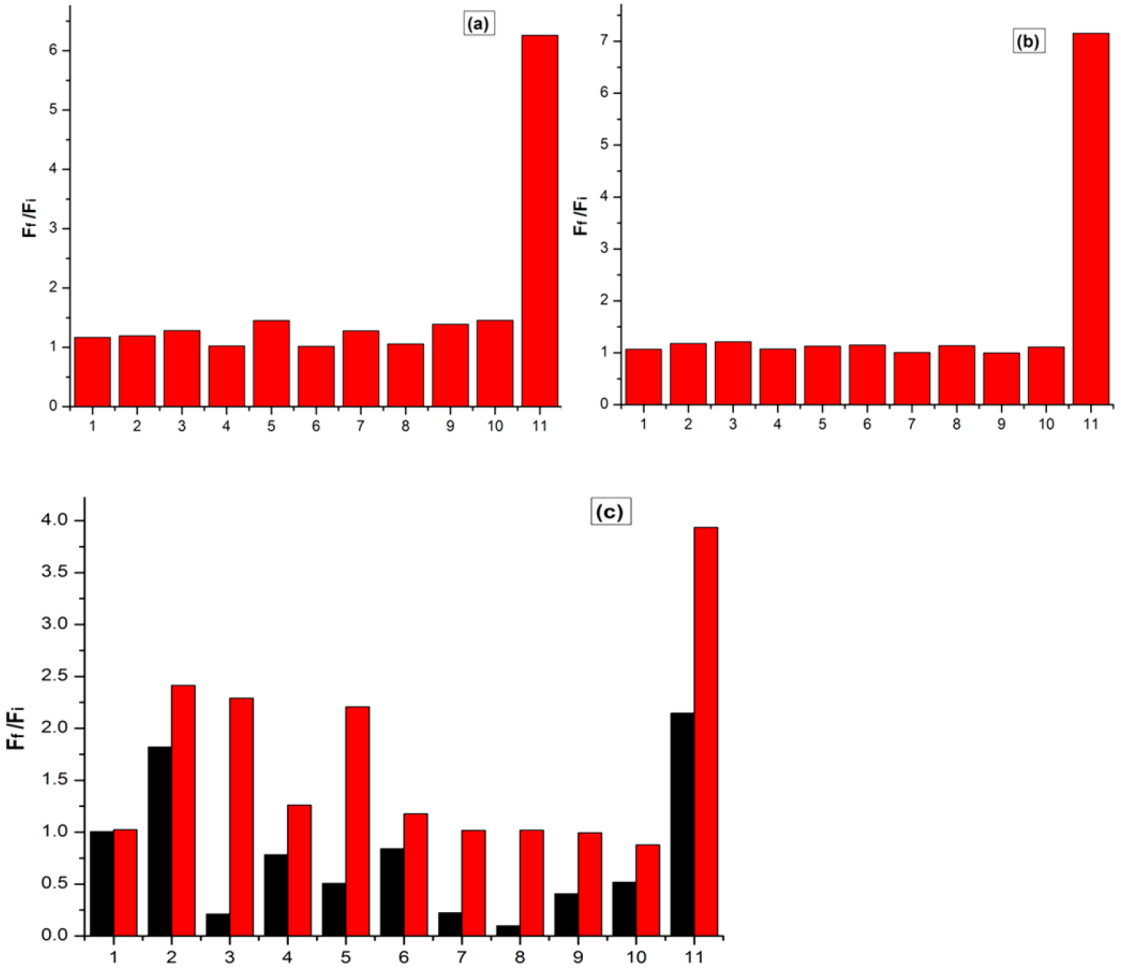

Figure 5. Fluorescence responses of SNAN-1, SNAN-2, and SNAN-3 to various RSONs in the order 1−11, glutathione, cysteine, α-lipoic acid (ALA), thiosulfate, sulfite, thiocyanate, nitrite, H_2O_2, hypochlorite (OCl^-), and H_2S: (a) 30 μM SNAN-1 at 408 nm, (b) 30 μM SNAN-2 at 410 nm, and (c) 5 μM SNAN-3 at 410 nm (black) and 540 nm (red) to various reactive sulfur, nitrogen, and oxygen species (RSONs) in 95:5 1× PBS (pH 7.4):DMSO (for SNAN-1 and 2), 90:10 1× PBS (pH 7.4):DMSO (for SNAN-3) with λ_{ex}= 350 nm. The bars represent responses after 120 min of analyte addition. For all comparisons, the data shown represent 500 μM glutathione, 500 μM cysteine, 100 μM other RSONs, and 30 μM H_2S for SNAN-1 and SNAN-2, 0.5 μM H_2S for 410 nm, and 50 μM H_2S for 540 nm measurements for SNAN-3.

were observed at different time points (Figure 4). From the spectra, it is evident that under the H_2S limiting conditions (0.5 μM), small changes were seen signifying the PET process. Under probe-limiting conditions (500 μM H_2S), a gradual decrease in the absorption maxima at 350 nm and the formation of new ICT absorption maxima were observed at 440 nm accompanied by the appearance of two isosbestic points at 320 and 390 nm.

On the basis of the fluorogenic signal enhancement of the SNAN-1, SNAN-2, and SNAN-3 with H_2S, we investigated their selectivity toward H_2S over other reactive sulfur, oxygen, and nitrogen species (RSONs) consisting of glutathione, cysteine, α-lipoic acid (ALA), thiosulfate, sulfite, thiocyanate, nitrite, H_2O_2, and hypochlorite (OCl^-) (Figure 5). Probes SNAN-1 and SNAN-2 showed almost no OFF−ON fluorescence responses to any of the RSONs. In comparison to SNAN-1 and SNAN-2, SNAN-3 displayed approximately 1.6-fold (540 nm) and 2.4-fold (410 nm) lower dichroic fluorescence turn ON ratios for sulfide. It should also be noted that SNAN-3 displayed higher background reactivity to other analytes at 540 nm and quenching at 410 nm (indicating the possible conversion from azide to amino). Glutathione, cysteine, and sulfite contributed the most to the observed background increase at 540 nm for SNAN-3. We observed that, SNAN-3 demonstrates greater signal diversity and exhibited two OFF−ON fluorescence signals. Altogether, these assays demonstrate the selectivity of all three SNAN probes toward the detection of sulfide in vitro.

■ CONCLUSIONS

In summary, we developed three reaction-based fluorescent probes for the detection of H_2S based on two new design platforms. In addition, a new approach in detecting H_2S by the reduction of azide to a triazene intermediate in aqueous media is reported. These chemodosimeters are based on selective chemical reactions that can be useful in triggering certain photophysical processes and provide novel insights into the relatively unexplored area of C_0 chemosensors. In light of the numerous examples involving *N*-alkyl-1,8-naphthalimides, this study demonstrates that the chemistry of *N*-aryl-1,8-naphthalimide is particularly useful in this regard because it allows for straightforward placement of the ICT and PET modulators on the same molecule. In the three examples presented, the *N*-aryl modification proved to be effective, as it allowed the placement of PET modulator at a strategically important and less explored imide position in 1,8-naphthalimides. Given the unique reaction mechanism of hydrogen sulfide reduction taken together with exceptionally long-lived intermediate from SNAN-2 demonstrated

DOI: 10.1021/acs.joc.7b01952
J. Org. Chem. 2017, 82, 12153−12161

by ^{1}H NMR, faster reaction kinetics from these electron-deficient fluorescent platforms should be possible with electron-releasing substituents. Substituents such as methoxy or dimethylamino should destabilize the intermediate; however, the potential for dual fluorescence may be diminished. These probes or dosimetric agents have demonstrated good selectivity, greater signal diversity, and the more desirable OFF−ON fluorescence response. To the best of our knowledge, probe SNAN-3 represents the only example showing a dual-emission and dual-channel optical response for the detection of sulfide in aqueous solution. Moreover, the probe remains the only H_2S detecting system that invokes both azido and nitro functional groups on the same fluorescent platform; the combination gives a surprising tandem set of concentration ranges at either probe-limiting or sulfide-limiting conditions. With hydrogen sulfide concentrations in human blood typically between 10 and 100 μM and living cells containing lower submicromolar concentration ranges, the detection limits of these probes, particularly SNAN-3 with a detection limit of between 0.1 and 0.5 μM, appear well-suited for cellular applications.[37] In light of these observations, we believe other reaction-based probes with built-in triggers for photophysical processes can be designed rationally using similar design platforms and will appear in due course. Furthermore, the differential responses from these probes indicate that 1,8-naphthalimide can be exploited in designing chemodosimeters that can be used in the detection of multiple analytes.

EXPERIMENTAL SECTION

General Information. Commercial reagents were used as received unless otherwise stated. Merck 60 silica gel was used for chromatography, and Whatman silica gel plates with fluorescence F254 were used for TLC analysis. ^{1}H NMR and ^{13}C NMR spectra for characterization of new compounds were collected in DMSO-d6 (Cambridge Isotope Laboratories, Cambridge, MA) at 25 °C on a Bruker Avance-400 spectrometer. Data for ^{1}H are reported as follows: chemical shift (ppm) and multiplicity (s = singlet, d = doublet, t = triplet, q = quartet, m = multiplet). Data for ^{13}C NMR are reported as ppm. High-resolution mass spectral analyses (ESI-MS; TOF Mass Analyzer) were carried out with a Waters/Micromass LCT Premier system at the UNM mass spectrometric facility. IR stretches are given in cm^{-1}; spectra were obtained on an Avatar 360 FT-IR.

Probes Syntheses. *4-Cyano-1,8-naphthalic anhydride (**1**).*

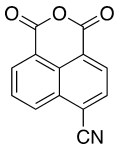

According to the published method,[54] 4-bromo-1,8-naphthalic anhydride (300 mg, 1.083 mmol) and CuCN (111.5 mg, 1.245 mmol) were taken in 2 mL dry DMF and heated at 150 °C for 8 h. After that, the reaction mixture was allowed to cool to 50 °C, and $FeCl_3{\cdot}6H_2O$ (0.6 g) (*Caution*! Generation of HCN from unreacted CuCN is expected, so a well-ventilated fume hood is recommended!) and 1.7 M HCl (1 mL) were added. The reaction mixture was stirred at this temperature for 15 min and then cooled to room temperature. Then, water was added; the mixture was stirred for 5 min, and the solids were filtered and washed with water and dried. The crude product obtained was recrystallized from acetone as pale yellow solid (164 mg, 68%).

^{1}H NMR (400 MHz, DMSO-d6) δ: 8.67 (d, J = 7.78 Hz, 1H), 8.6 (m, 2H), 8.5 (d, J = 7.53 Hz, 1H), 7.95 (t, J = 7.53 Hz, 1H). ^{13}C NMR (100 MHz, DMSO-d6) δ: 160.4, 160.2, 134.5, 133.8, 131.8, 131.2, 130.7, 129.7, 124.1, 120.7, 116.6, 115.3.

General Procedure for the Syntheses of Compounds 4, 5, and 6.[55] One millimole of naphthalic anhydride and 1.1 equiv of *p*-phenylenediamine were taken in 25 mL of ethanol and refluxed for 12 h. Then, the reaction mixture was filtered warm to collect the formed precipitate, which then was washed with ethanol and dried. The obtained product was pure and used for the next step without any further purification.

*2-(4-Aminophenyl)-6-cyano-1H-benzo[de]isoquinoline-1,3(2H)-dione (**4**).*

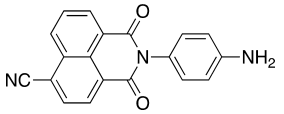

Pale orange solid, yield: 191 mg (61%); ^{1}H NMR (400 MHz, DMSO-d6) δ: 8.62−8.47 (m, 4H), 8.12 (t, J = 8.03 Hz, 1H), 6.97 (d, J = 8.53 Hz, 2H), 6.65 (d, J = 8.53 Hz, 2H), 5.28 (bs, 2H, NH_2). ^{13}C NMR (100 MHz, DMSO-d6) δ: 163.9, 163.5, 149.2, 134.4, 132.3, 130.8, 130.5, 129.8, 129.5, 127.9, 127.5, 124.2, 123.8, 117.0, 114.4, 114.2. IR (cm^{-1}): 3368, 3355, 2210, 1710, 1665, 1517, 1238. Mp: 360−362 °C.

*2-(4-Aminophenyl)-6-chloro-1H-benzo[de]isoquinoline-1,3(2H)-dione (**5**).*

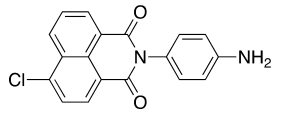

White solid, yield: 193 mg (60%); ^{1}H NMR (400 MHz, DMSO-d6) δ: 8.62−8.47 (m, 4H), 8.02 (t, J = 8.03 Hz, 1H), 6.94 (d, J = 8.53 Hz, 2H), 6.65 (d, J = 8.53 Hz, 2H), 5.26 (bs, 2H, NH_2). ^{13}C NMR (100 MHz, DMSO-d6) δ: 164.1, 163.8, 149.1, 137.8, 132.1, 131.3, 130.5, 129.6, 129.2, 129.1, 129.0, 128.2, 124.0, 123.9, 122.6, 114.2. IR (cm^{-1}): 3463, 3364, 1704, 1659, 1238. Mp: 320−322 °C

*2-(4-Aminophenyl)-6-nitro-1H-benzo[de]isoquinoline-1,3(2H)-dione (**6**).*

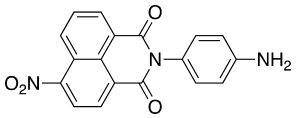

Red solid, yield: 203 mg (61%); ^{1}H NMR (400 MHz, DMSO-d6) δ: 8.73 (d, J = 8.78 Hz), 8.63−8.55 (m, 3H), 8.11 (t, J = 8.78 Hz, 1H), 6.97 (d, J = 8.78 Hz, 2H), 6.64 (d, J = 8.78 Hz, 2H), 5.30 (bs, 2H, NH_2). ^{13}C NMR (100 MHz, DMSO-d6) δ: 164.0, 163.2, 149.6, 149.1, 132.2, 130.6, 130.1, 129.5, 129.1, 129.1, 127.8, 124.7, 123.8, 123.7, 123.3, 114.2. IR (cm^{-1}): 3413, 1704, 1661, 1523, 1516, 1349, 1239. Mp: 300−302 °C.

General Procedure for the Syntheses of SNAN-1, 2, and 3.[56] To a solution of 0.3 mmol amine and 9 equiv of *p*-toluene sulfonic acid monohydrate in 2 mL of water was added 9 equiv of sodium nitrite slowly over 15 min. The resulted suspension was stirred at room temperature for 2 h. Then, 1.6 equiv of sodium azide (*Caution*! Hydrazoic acid might be generated, so the reaction should be performed in fumehood) was added, and the reaction mixture was stirred for another 90 min. Then water was added, and the precipitate was filtered and washed with water and dried. The crude product was purified by silica column chromatography using 80% dichloromethane in hexane.

2-(4-Azidophenyl)-6-cyano-1H-benzo[de]isoquinoline-1,3(2H)-dione (SNAN-1).

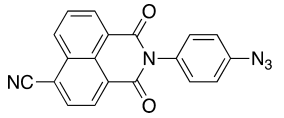

White solid, yield: 55 mg (54%); ^{1}H NMR (400 MHz, DMSO-d6) δ: 8.64−8.50 (m, 4H), 8.15 (t, J = 8.28 Hz, 1H), 7.44 (d, J = 8.78 Hz, 2H), 7.28 (d, J = 8.78 Hz, 2H). ^{13}C NMR (100 MHz, DMSO-d6) δ: 163.6, 163.3, 140.0, 134.4, 132.8, 132.3, 131.1, 130.9, 130.8, 130.5, 129.8, 128.0, 127.4, 124.1, 120.1, 117.0, 114.6. IR (cm^{-1}): 2230, 2128, 1716, 1677, 1593, 1508, 1237. Mp: 270−272 °C (decomposed). HRMS (ESI-TOF) m/z: [M]+ Calcd for $C_{19}H_9N_5O_2$: 339.0756. Found 339.3071

DOI: 10.1021/acs.joc.7b01952
J. Org. Chem. 2017, 82, 12153−12161

2-(4-Azidophenyl)-6-chloro-1H-benzo[de]isoquinoline-1,3(2H)-dione (SNAN-2).

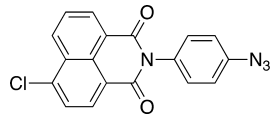

White solid, yield: 75 mg (72%); ^{1}H NMR (400 MHz, DMSO-d6) δ: 8.66 (d, J = 8.53 Hz, 1H), 8.58 (d, J = 8.53 Hz, 1H), 8.43 (d, J = 8.53 Hz, 1H), 8.07−8.01 (m, 2H), 7.42 (d, J = 8.53 Hz, 2H), 7.26 (d, J = 8.53 Hz, 2H). ^{13}C NMR (100 MHz, DMSO-d6) δ: 163.9, 163.6, 139.9, 138.1, 132.9, 132.2, 131.5, 131.1, 130.8, 129.3, 129.2, 129.1, 128.2, 123.7, 122.4, 120.1. IR (cm^{-1}): 2120, 1707, 1669, 1508, 1233. Mp: 218−220 °C (decomposed). HRMS (ESI-TOF) m/z: [M]+ Calcd for $C_{18}H_9ClN_4O_2$ 348.0414. Found 348.7427.

2-(4-Azidophenyl)-6-nitro-1H-benzo[de]isoquinoline-1,3(2H)-dione (SNAN-3).

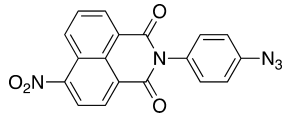

Pale yellow solid, yield: 59 mg (61%) ^{1}H NMR (400 MHz, DMSO-d6) δ: 8.76 (d, J = 8.53 Hz, 1H), 8.66−8.58 (m, 3 H), 8.13 (t, J = 7.53 Hz, 1H), 7.46 (d, J = 8.78 Hz, 2H), 7.29 (d, J = 8.78 Hz, 2H). ^{13}C NMR (100 MHz, DMSO-d6) δ: 163.8, 163.0, 149.0, 140.0, 132.8, 132.2, 131.1, 130.6, 130.1, 129.4, 129.3, 127.7, 124.7, 123.8, 123.3, 120.1. IR (cm^{-1}): 2113, 1711, 1664, 1529, 1507, 1346, 1238. Mp: 210−212 °C (decomposed). HRMS (ESI-TOF) m/z: [M]+ Calcd for $C_{18}H_9N_5O_4$ 359.0655 Found 359.2952.

6-Amino-2-(4-aminophenyl)-1H-benzo[de]isoquinoline-1,3(2H)-dione (7).

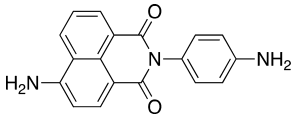

Compound 7 was synthesized according to the literature procedure.[56] Dark green solid based on 1.0 mmol preparation; yield: 243 mg (61%). ^{1}H NMR (400 MHz, DMSO-d6) δ: 8.62 (d, J = 7.92 Hz, 1H), 8.39 (d, J = 7.08 Hz, 1H), 8.16 (d, J = 8.48 Hz, 1H), 7.65 (t, J = 7.84 Hz, 1H), 7.44 (s, 2H), 6.85 (d, J = 8.04 Hz, 2H), 6.61 (d, J = 7.88 Hz, 2H), 5.22 (bs, 2H, NH_2). ^{13}C NMR (100 MHz, DMSO-d6) δ: 164.8, 164.0, 153.1, 148.7, 134.4, 131.5, 130.5, 129.7, 124.9, 124.5, 122.8, 119.9, 114.2, 108.6, 108.5. IR (cm^{-1}): 3427, 3346, 3235, 2920, 2844, 1672, 1637, 1613, 1572, 1368, 1246. Mp: 364−366 °C.

■ ASSOCIATED CONTENT

Supporting Information

The Supporting Information is available free of charge on the ACS Publications website at DOI: 10.1021/acs.joc.7b01952.

^{1}H and ^{13}C NMR spectra, fluorescence spectra, mechanistic scheme for H_2S reduction, HRMS plots for probes SNAN-1, SNAN-2, and SNAN-3 (PDF)

■ AUTHOR INFORMATION

Corresponding Author

*E-mail: mheagy@nmt.edu.

ORCID

Michael D. Heagy: 0000-0002-4519-078X

Notes

The authors declare no competing financial interest.

■ ACKNOWLEDGMENTS

NSF Award IIA-1301346 is acknowledged for support of fluorescence spectroscopy instrumentation. M.D.H. wishes to thank Dr. Virginia Chang for her assistance in obtaining the NMR data.

■ REFERENCES

(1) Pryor, W. A.; Houk, K. N.; Foote, C. S.; Fukuto, J. M.; Ignarro, L. J.; Squadrito, G. L.; Davies, K. J. *American Journal of Physiology-Regulatory, Integrative and Comparative Physiology* **2006**, *291* (3), R491.
(2) Chen, C. Q.; Xin, H.; Zhu, Y. Z. *Acta Pharmacol. Sin.* **2007**, *28*, 1709−1716.
(3) Qu, K.; Lee, S. W.; Bian, J. S.; Low, C. M.; Wong, P. T. *Neurochem. Int.* **2008**, *52*, 155−165.
(4) Gadalla, M. M.; Snyder, S. H. *J. Neurochem.* **2010**, *113*, 14−26.
(5) Kabil, O.; Banerjee, R. *J. Biol. Chem.* **2010**, *285*, 21903−21907.
(6) Mancuso, C.; Navarra, P.; Preziosi, P. *J. Neurochem.* **2010**, *113*, 563−575.
(7) Wang, R. *Physiol. Rev.* **2012**, *92*, 791−896.
(8) Paul, B. D.; Snyder, S. H. *Nat. Rev. Mol. Cell Biol.* **2012**, *13*, 499−507.
(9) Lindenmann, J.; Matzi, V.; Neuboeck, N.; Ratzenhofer-Komenda, B.; Maier, A. *Diving Hyperb Med.* **2010**, *40*, 213−217.
(10) Wallace, K. J.; Cordero, S. R.; Tan, C. P.; Lynch, V. M.; Anslyn, E. V. *Sens. Actuators, B* **2007**, *120*, 362−367.
(11) Huang, D.; Xu, B.; Tang, J.; Luo, J.; Chen, L.; Yang, L.; Yang, Z.; Bi, S. *Anal. Methods* **2010**, *2*, 154−158.
(12) Lawrence, N. S.; Davis, J.; Compton, R. G. *Talanta* **2000**, *52*, 771−784.
(13) Fogo, J. K.; Popowsky, M. Spectrophotometric Determination of Hydrogen Sulfide. *Anal. Chem.* **1949**, *21*, 732−734.
(14) Brunner, U.; Chasteen, T. G.; Ferloni, P.; Bachofen, R. *Chromatographia* **1995**, *40*, 399−403.
(15) Manibalan, K.; Mani, V.; Chang, P.-C.; Huang, C.-H.; Huang, S.-T.; Marchlewicz, K.; Neethirajan, S. *Biosens. Bioelectron.* **2017**, *96*, 233−238.
(16) Doeller, J. E.; Isbell, T. S.; Benavides, G.; Koenitzer, J.; Patel, H.; Patel, R. P.; Lancaster, J. R., Jr.; Darley-Usmar, V. M.; Kraus, D. W. *Anal. Biochem.* **2005**, *341*, 40−51.
(17) Esfandyarpour, B.; Mohajerzadeh, S.; Khodadadi, A. A.; Robertson, M. D. *IEEE Sens. J.* **2004**, *4*, 449−454.
(18) Ishigami, M.; Hiraki, K.; Umemura, K.; Ogasawara, Y.; Ishii, K.; Kimura, H. *Antioxid. Redox Signaling* **2009**, *11*, 205−214.
(19) Furne, J.; Saeed, A.; Levitt, M. D. *Am. J. Physiol Regul Integr Comp Physiol* **2008**, *295*, R1479−R1485.
(20) Han, Y.; Qin, J.; Chang, X.; Yang, Z.; Du, J. *Cell. Mol. Neurobiol.* **2006**, *26*, 101−107.
(21) Warenycia, M. W.; Goodwin, L. R.; Benishin, C. G.; Reiffenstein, R. J.; Francom, D. M.; Taylor, J. D.; Dieken, F. P. *Biochem. Pharmacol.* **1989**, *38*, 973−981.
(22) Chan, J.; Dodani, S. C.; Chang, C. J. *Nat. Chem.* **2012**, *4*, 973−984.
(23) Jun, M. E.; Roy, B.; Ahn, K. H. *Chem. Commun.* **2011**, *47*, 7583−7601.
(24) Yu, F.; Han, X.; Chen, L. *Chem. Commun.* **2014**, *50*, 12234−12249.
(25) Peng, H.; Cheng, Y.; Dai, C.; King, A. L. *Angew. Chem., Int. Ed.* **2011**, *50* (41), 9672−9675.
(26) Qian, Y.; Karpus, J.; Kabil, O.; Zhang, S. Y.; Zhu, H. L.; Banerjee, R.; Zhao, J.; He, C. *Nat. Commun.* **2011**, *2*, 495 Article 495..
(27) Qian, Y.; Zhang, L.; Ding, S.; Deng, X.; He, C.; Zheng, X. E.; Zhu, H.-L.; Zhao, J. *Chem. Sci.* **2012**, *3*, 2920−2923.
(28) Saha, T.; Kand, D.; Talukdar, P. *Org. Biomol. Chem.* **2013**, *11*, 8166−8170.
(29) Duke, R. M.; Veale, E. B.; Pfeffer, F. M.; Kruger, P. E.; Gunnlaugsson, T. *Chem. Soc. Rev.* **2010**, *39*, 3936−3953.
(30) Wang, M.; Xu, Z.; Wang, X.; Cui, J. *Dyes Pigm.* **2013**, *96*, 333−337.
(31) Xu, Z.; Han, S. J.; Lee, C.; Yoon, J.; Spring, D. R. *Chem. Commun.* **2010**, *46*, 1679−1681.
(32) Xu, Z.; Qian, X.; Cui, J. *Org. Lett.* **2005**, *7*, 3029−3032.

DOI: 10.1021/acs.joc.7b01952
J. Org. Chem. 2017, 82, 12153−12161

(33) Xu, Z.; Xiao, Y.; Qian, X.; Cui, J.; Cui, D. *Org. Lett.* **2005**, *7*, 889−892.
(34) Guo, Y.; Zeng, T.; Shi, G.; Cai, Y.; Xie, R. *RSC Adv.* **2014**, *4*, 33626−33628.
(35) Montoya, L. A.; Pluth, M. D. *Chem. Commun.* **2012**, *48*, 4767−4769.
(36) Shi, D. T.; Zhou, D.; Zang, Y.; Li, J.; Chen, G. R.; James, T. D.; He, X. P.; Tian, H. *Chem. Commun.* **2015**, *51*, 3653−3655.
(37) Xuan, W.; Pan, R.; Cao, Y.; Liu, K.; Wang, W. *Chem. Commun.* **2012**, *48*, 10669−10671.
(38) He, L.; Lin, W.; Xu, Q.; Wei, H. *Chem. Commun.* **2015**, *51*, 1510−1513.
(39) Kim, G.; Jang, E.; Page, A. M.; Ding, T.; Carlson, K. A.; Cao, H. *RSC Adv.* **2016**, *6*, 95920−95924.
(40) Liu, T.; Xu, Z.; Spring, D. R.; Cui, J. *Org. Lett.* **2013**, *15*, 2310−2313.
(41) Zieschang, F.; Schreck, M. H.; Schmiedel, A.; Holzapfel, M.; Klein, J. H.; Walter, C.; Engels, B.; Lambert, C. *J. Phys. Chem. C* **2014**, *118*, 27698−27714.
(42) de Silva, A. P.; de Silva, S. A. *J. Chem. Soc., Chem. Commun.* **1986**, *23*, 1709−1710.
(43) de Silva, A. P.; Rupasinghe, R. A. D. D. *J. Chem. Soc., Chem. Commun.* **1985**, 1669−1670.
(44) Czarnik, A. W. *Acc. Chem. Res.* **1994**, *27*, 302−308.
(45) Huston, M. E.; Haider, K. W.; Czarnik, A. W. *J. Am. Chem. Soc.* **1988**, *110*, 4460−4462.
(46) Wang, R.; Yu, F.; Chen, L.; Chen, H.; Wang, L.; Zhang, W. *Chem. Commun.* **2012**, *48*, 11757−11759.
(47) Bamesberger, A.; Schwartz, C.; Song, Q.; Han, W.; Wang, Z.; Cao, H. *New J. Chem.* **2014**, *38*, 884−888.
(48) Cao, H.; Chang, V.; Hernandez, R.; Heagy, M. D. *J. Org. Chem.* **2005**, *70*, 4929−4934.
(49) Cao, H.; Diaz, D. I.; DiCesare, N.; Lakowicz, J. R.; Heagy, M. D. *Org. Lett.* **2002**, *4*, 1503−1505.
(50) Wang, J.; Yang, L.; Hou, C.; Cao, H. *Org. Biomol. Chem.* **2012**, *10*, 6271−6274.
(51) Takahashi, S.; Nozaki, K.; Kozaki, M.; Suzuki, S.; Keyaki, K.; Ichimura, A.; Matsushita, T.; Okada, K. *J. Phys. Chem. A* **2008**, *112*, 2533−2542.
(52) Nandhikonda, P.; Begaye, M. P.; Cao, Z.; Heagy, M. D. *Chem. Commun.* **2009**, 4941−4943.
(53) Nandhikonda, P.; Begaye, M. P.; Cao, Z.; Heagy, M. D. *Org. Biomol. Chem.* **2010**, *8*, 3195−3201.
(54) Friedman, L.; Shechter, H. *J. Org. Chem.* **1961**, *26*, 2522−2524.
(55) Greenfield, S. R.; Svec, W. A.; Gosztola, D.; Wasielewski, M. R. *J. Am. Chem. Soc.* **1996**, *118*, 6767−6777.
(56) Kutonova, K. V.; Trusova, M. E.; Postnikov, P. S.; Filimonov, V. D.; Parello, J. A. *Synthesis* **2013**, *45*, 2706−2710.
(57) Gunnlaugsson, T.; Kruger, P. E.; Jensen, P.; Pfeffer, F. M.; Hussey, G. M. *Tetrahedron Lett.* **2003**, *44*, 8909−8913.
(58) Bissell, R. A.; de Silva, A. P.; Gunaratne, H. Q. N.; Lynch, P. L. M.; Maguire, G. E. M.; Sandanayake, K. R. A. S. *Chem. Soc. Rev.* **1992**, *21*, 187−195.
(59) Bissell, R. A.; de Silva, A. P.; Nimal Gunaratne, H. Q.; Mark Lynch, P. L.; Maguire, G. E. M.; McCoy, C. P.; Samankumara Sandanayake, K. R. A.S.. Fluorescent PET (photoinduced electron transfer) sensors. In *Photoinduced Electron Transfer V*; Mattay, J., Ed.; Springer Berlin Heidelberg: Berlin, Heidelberg, 1993; p 223.
(60) Veale, E. B.; Tocci, G. M.; Pfeffer, F. M.; Kruger, P. E.; Gunnlaugsson, T. *Org. Biomol. Chem.* **2009**, *7*, 3447−3454.
(61) Henthorn, H. A.; Pluth, M. D. *J. Am. Chem. Soc.* **2015**, *137*, 15330−15336.
(62) Bozdemir, O. A.; Guliyev, R.; Buyukcakir, O.; Selcuk, S.; Kolemen, S.; Gulseren, G.; Nalbantoglu, T.; Boyaci, H.; Akkaya, E. U. *J. Am. Chem. Soc.* **2010**, *132*, 8029−8036.
(63) de Silva, A. P.; McClenaghan, N. D. *Chem. - Eur. J.* **2002**, *8*, 4935−4945.
(64) Demchenko, A. P. *Lab Chip* **2005**, *5*, 1210−1223.
(65) Demchenko, A. P. *J. Fluoresc.* **2010**, *20*, 1099−1128.
(66) Ueno, T.; Urano, Y.; Kojima, H.; Nagano, T. *J. Am. Chem. Soc.* **2006**, *128* (33), 10640−10641.
(67) Lakowicz, J. R. Instrumentation for Fluorescence Spectroscopy. In *Principles of Fluorescence Spectroscopy*; Lakowicz, J. R., Ed.; Springer US: Boston, MA, 2006; p 27.
(68) Wintgens, V.; Valat, P.; Kossanyi, J.; Demeter, A.; Biczok, L.; Berces, T. *New J. Chem.* **1996**, *20*, 1149−1158.

DOI: 10.1021/acs.joc.7b01952
J. Org. Chem. 2017, 82, 12153−12161